

THE TRANSITION PROCESS FROM LAMINAR TO TURBULENT FLOW

HORIA DUMITRESCU¹, VLADIMIR CARDOS¹ AND RADU BOGATEANU²

¹“Gheorghe Mihoc – Caius Iacob” Institute of Mathematical Statistics and Applied Mathematics of the Romanian Academy
Calea 13 Septembrie no. 13, 050711 Bucharest, Romania
dumitrescu.horia@yahoo.com, v_cardos@yahoo.ca, www.ima.ro

² INCAS - National Institute for Aerospace Research "Elie Carafoli", Bucharest, Bd. Iuliu Maniu 220,
E-mail: unquradu@gmail.com, bogateanu.radu@incas.ro, www.incas.ro

Key words: Laminar-turbulent Transition, Shear Turbulence, Twisted Disc Model, Contact Structure.

Abstract. It is commonly assumed that the transition process from laminar to turbulent flow occurs because of an incipient instability of the basic flow field. This non-defined instability depending on subtle and obscure details of the free flow enters the boundary layer from where a variety of different instabilities can occur and grow up to the breakdown of laminar flow. The scenario following various linear stability approaches within a framework of the classical Navier-Stokes theory however failed to explain the origin and the mechanism of the transition process. The “original sin” lies just in the ignorance of the initial impulse triggering off an instability state. In the paper, this drawback is removed in the sense that any flow is started at some moment in time from rest, where the initial impulse/starting impact has occurred, and as long as the Reynolds number (or a similar stability parameter λ) doesn't exceed a critical value, the flow/motion remains laminar/elastic regime. The wall-bounded motion, both for solids and fluids, is a rotor-translational motion creating permanently an instability state firstly in the linear/elastic range, and then followed by transition to non-linear instabilities at a critical threshold and a statistical/hysteretic damping state. By means of the model of rotor-translational motion, a universal stability parameter depending on the starting impact (V_∞^2) is defined where such as parameter is the boundary Reynolds number $Rb = e^\tau v^{1/\tau} / V_\infty^2$, (with e^τ - the concentrated boundary vorticity, $v^{1/\tau}$ - the kinematic viscosity, $\tau \leq 2$ - a torsion index) for fluids and the wave number $k = \pi/2 + n\pi$, ($n = 1, 2, 3$) for solids.

1 INTRODUCTION

When the Reynolds is increased, the flows of real fluids differ from the quiet smooth flows known as laminar flows, and their opposite, either internal flows or boundary layers adjacent to solid surfaces undergo a spectacular transition process from the laminar to the turbulent regime. In the turbulent flows the vorticity, pressure, temperature and other fluid mechanical quantities fluctuate in an observable disordered-manner with extremely sharp and irregular space and time variations. The observation that the orderly pattern of flow ceases to exist at higher Reynolds

numbers, and that the flow through a pipe becomes turbulent was firstly shown by O. Reynolds [1]. Unlike other complicated phenomena, turbulence is easily observed, but is extremely difficult to interpret, understand, explain and non in the last place to simulate. Since the turbulence dynamics is a rapid process originated at the fluid-solid boundary interface ($y \rightarrow 0$) laying in packets of vorticity/shear waves caused by the onset of motion [2], the classical approaches based on the Navier-Stokes equations (N-S equations for short) with Stokes ($\lambda = -2/3\mu$) and Prandtl (constant viscosity μ) hypotheses could statistically describe (URANS, LES computations) only large-scale slow phenomena “en mass”. The true problem of turbulence dynamics generated by high frequency wall-vorticity waves, requests a new formulation of N-S equations near the wall, for taking into account the effects of twisted flow during the starting impact: the concentrated/twisted boundary vorticity (CVB) and the non-linear behavior of fluid (the thixotropic fluid hypothesis, $\nu(\text{Re}_l)$) [2]. However, since such a formulation is not available at this time, the whole flow field is described by the soliton solutions derived from similar solutions (localizing boundary singularities) associated with a mutual induction function, $\text{CBV} - \nu(\text{Re}_l)$, acting as a substitute for the Stokes’s hypothesis which annihilates the turbulent solutions; *i.e. valid Stokes’s hypothesis, no solution for turbulence exists*. The soliton solutions exhibit both average flow field and wavy flow pattern frozen at a given instant (*i.e.* relativity effects) and transported by the main motion as a whole [2],[3].

2 THE PHYSICAL NATURE OF VORTICITY AT A SOLID BOUNDARY

The vorticity is a kinematical quantity and the equation governing its evolution, known as Helmholtz’s vorticity transport equation, is derived from the N-S equation by a purely mathematical operation, so that this contains the same restriction as the original N-S equation, based indirectly on the concept of the point material excluding any inertial rotatory effect. The most primary derived fields that describe the local spatial variation of a velocity field \mathbf{u} are its divergence ($\nabla \cdot \mathbf{u}$), a scalar field called dilatation and its curl ($\nabla \times \mathbf{u}$), an axial vector called vorticity. The dilatation measures the expansion or compression of the fluid, while the vorticity measures the rotation of fluid particles, as sketched in Fig. 1.

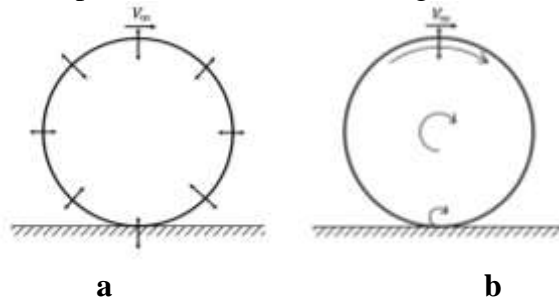


Figure1: The velocity field associated with: a) dilatation – compressing/ expanding process and b) vorticity - shearing process at the wall.

Thus, the dilatation represents an isotropic compressing process, while the vorticity is a non-isotropic shearing process. The effort to explain vortical flows as diversely as possible, by means of coupling of compressing and shearing processes into a unitary approach [4], was not very successful: vorticity-creation from the wall. The shear turbulence processes remain further

unknown as long as the fluid is assumed ideal or Newtonian; *i.e. no-elasticity shear in fluid, no turbulence exists.*

Historically, the viscosity property of fluid was used by Stokes [5] in the famous Navier-Stokes equation (NSE) as an intrinsic relation between the first and second viscosities ($3\lambda + \mu = 0$), for reducing the number of properties which characterizes the field of stresses in a flowing compressible fluid. The ignorance of the physical interpretation of the Stokes's hypothesis has lead to the much disputed problem concerning the NSE solutions [6]. After half a century, the practical importance of NSE was proved for solving d'Alembert's paradox (D – drag crisis) by means of another famous mathematical development, Prandtl's boundary layer theory [7]. But, in spite of these heaviest and the most ambitious armory from theoretical physics and mathematics, the solution of the full time-dependent 3D NSE for turbulent flows is far (or impossible) from being found. The big mathematical problem of turbulence remains unsolved as a new challenge in Fluid Dynamics, T – turbulence paradox. Indeed, the approach of turbulence via the NSE with the Stokes approximation disregards the detailed wall-bounded flow structure at the starting moment ($y=0, t \rightarrow 0$), where the initial and boundary conditions, $\mathbf{u}(0, t) = 0$ (no slip condition) and $v \equiv \mu/\rho = v_0$ (equilibrium value) corresponds exactly to one flow state called Blasius flow. The Stokes relation associated with the incompressible flow assumption ($\rho = \text{const.}$) obscure the easiest compressibility effects occurred during the short starting time ($t \rightarrow 0$) at the solid boundary, *acting like a fluid-solid collision called the starting impact [2].*

After impact, any flowing incompressible flow has a more or less non-constant/elastic shear viscosity at solid boundaries, and whereby the shearing is also a universal process causing transverse waves that expands in the boundary-layer flow; when the Reynolds exceeds a critical value, the shearing process becomes a self-sustaining one, generating vortices.

3 THE DYNAMIC MODEL OF STARTING IMPACT-ROTOR-TRANSLATION MOTION AT WALL

Among various wall-bounded flows at large Reynolds numbers, the primary observable structure is thin boundary layers generated by and adjacent to solid surfaces. In these vortical flows generated by a moving body, the formation and evolution of boundary layer are closely related to the vorticity-creation process at a solid surface during the onset of motion.

The motion at impact ($t \rightarrow 0$). Even if a flow is incompressible, its starting produces weak compressibility effects with important consequences concerning the motion following start up. The flow of a gas can be considered incompressible when the relative change in density remains

very small, $\Delta\rho/\rho_0 \ll 1/2 \left(\frac{V_\infty}{c}\right)^2 = 1/2M_\infty^2$, and in the case of air usually a value of $M_\infty = \sqrt{0.1} \approx 1/3$ or 100 m/s can be considered as an incompressibility limit.

However, for $V_\infty = 100 \text{ m/s}$ and $l = 1$, the Reynolds number ($Re_l = 2/3 \cdot 10^7$) exceeds its critical value, that is the flow is fully turbulent where there is the possibility that in starting condition ($t = 0$) the easy/early compressibility effects cause the oscillating behavior of viscosity and associated with an inherent fluctuating velocity field, near solid surfaces, produce a self-sustaining non-stationary flow termed generic shear turbulence [2]. Figure 2 shows the dependence of elastic shear viscosity due to the early compressibility effects in wall-bounded

flows, where the crests of the longitudinal compressing/expanding process propagate with the group velocity $M_g = 2/3$. The Reynolds number has a more general interpretation of the classical parameter as a stability standard/control parameter of the flow state (the flow is stable for $Re_l \leq Re_c$ and unstable for $Re_l > Re_c$), and the Reynolds number is also a current reduced frequency for all real fluid motions.

$$Re_l \equiv \frac{V_\infty l}{\nu_0} = \frac{V_\infty^2 \nu_0^{-1}}{V_\infty / l} = \frac{\text{frequency of wall-bounded flow}}{\text{frequency of outer flow}}.$$

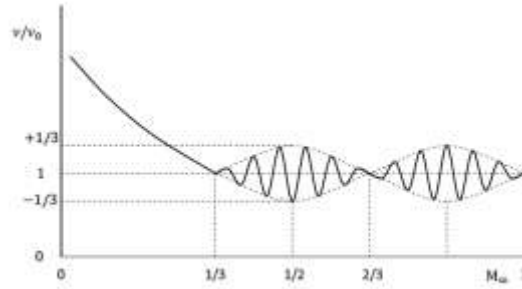


Figure 2: Elasticity effect in thixotropic fluid (longitudinal compressing/expanding process).

Then, we define the start-up by the impulsive phase change from the natural translational motion to a pure shear straining rotational motion (i.e. in the limit of vanishing contacting time) with no-loss of mass, energy and momentum, as sketched in Fig. 3.

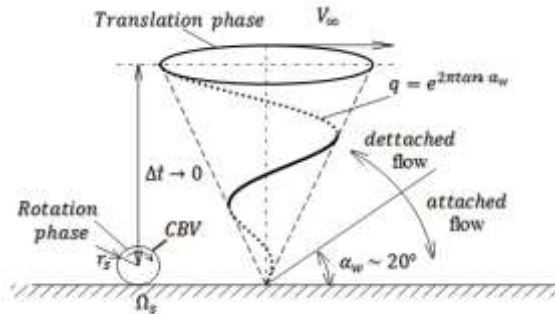


Figure 3: The impulsive phase change during the start-up with equal-energy partition condition (transverse shearing process)

During the starting impact, the initial velocity distribution is rapidly changed and the result of the coupling of some compressing and shearing processes is the creation of concentrated vorticity balls at solid surfaces as

$$\lim_{v(t) \rightarrow 0} \frac{1}{V} \int_{\partial V} \theta \boldsymbol{\omega} \cdot \mathbf{n}_s dS \equiv \frac{p_{w,torsion}}{\rho V_\infty^2} = \frac{e^\tau \nu}{V_\infty^2},$$

where e is the CBV, ν is the kinematic shear viscosity of the thixotropic fluid adjusting itself mutually according to the stress state of flow, $\tau \in [2 - (-2)]$ is the concentration/torsion index

showing the twisting degree of flow, and $p_{w,torsion}$ is the wall-perturbed pressure, generally greater than the pressure of free flow, termed torsion pressure [8].

The essence of starting impact is: (1) the creation of twisted contact structures, like the CBV, through a fast compressing-shearing rotation process, accumulating internal/intrinsic energy in the form of inertial rotation potential; (2) the partition of post-impact motion in the proportion of 1/3 pure straining rotation and 2/3 natural translation is universal feature for any plane motion of restricted continuous media; (3) the wall-bounded motion after impact is a rotor-translational motion with two invariants: a kinematic one $V_\infty / r\Omega = 2$, and a dynamic other $2V_\infty^2 / r^2 \Omega^2 = 3 \approx \pi$ (azimuthal wavelength), which is a measure of twisted boundary vorticity.

The two properties of the thixotropic fluid, CBV (e^τ) and shear viscosity (v), have opposite tendencies “return force”/shearing process and “rotational inertia”/compressing process, where the wall torsion/twisted pressure must obey the law of equal action and reaction in the form of an equal-energy condition

$$e^\tau v / V_\infty^2 \equiv 1. \quad (1)$$

The outcome of Eq. (1) expresses a gross dynamic balance governing the whole dynamic process of motion. Physically, the wall torsion pressure is a rotatory energy, where the fluid strained by the wall has rather a solid body-like behavior with angular velocity e^τ and angular momentum v . Since their product must be equal to the kinetic energy $\rho/2V_\infty^2$, the wall torsion pressure excepting of a scale factor l^2 defines a boundary Reynolds number (per m^2) which is a kind of normal angular acceleration,

$$Rb \equiv e^\tau v / l^2 \left[s^{-2} \right]. \quad (2)$$

In contrast to the well-known Reynolds number Re_l which is a control parameter of flow state, this new boundary Reynolds number Rb is an order parameter switching the flow state. Its critical value,

$$Rb_{cr} = e^2 v_0^{-1}, v_0^{-1} - \text{the natural frequency of thixotropic fluid,} \quad (3)$$

is a non-rolling condition for the CBV, which separates the non-periodic creeping motion/laminar flow from the non-linear torsional vibration motion/turbulent flow.

The parameter Rb is an autonomous parameter depending only on the intrinsic state of fluid at the wall, where a first approximation of the starting condition of equal-partition of energies, (Eq.1), is $Rb = Re_l$. Using the end properties of the thixotropic fluid ($e^2, 1; 1, v_0$) and the approximation $Rb = Re_l$, the parameter Rb describing the local state of fluid can be predicted by means of three power law-like relationships, depending on the intensity of starting impact [2] as

$$e^\tau \left(v_0^{-1} \right)^{\frac{1}{1+\tau}}, \tau \in \{2, 1, 0\} \text{ for the inelastic impact,} \quad (4a)$$

$$e^\tau v_0^{-1}, \tau \in \{0, 1, 2\} \text{ for the linear/elastic impact,} \quad (4b)$$

$$e^{-\tau} (v_0^{-1})^{\frac{3}{2}}, \tau \in \left\{2, 1, \frac{1}{2}\right\} \text{ for the nonlinear/ballistic impact.} \quad (4c)$$

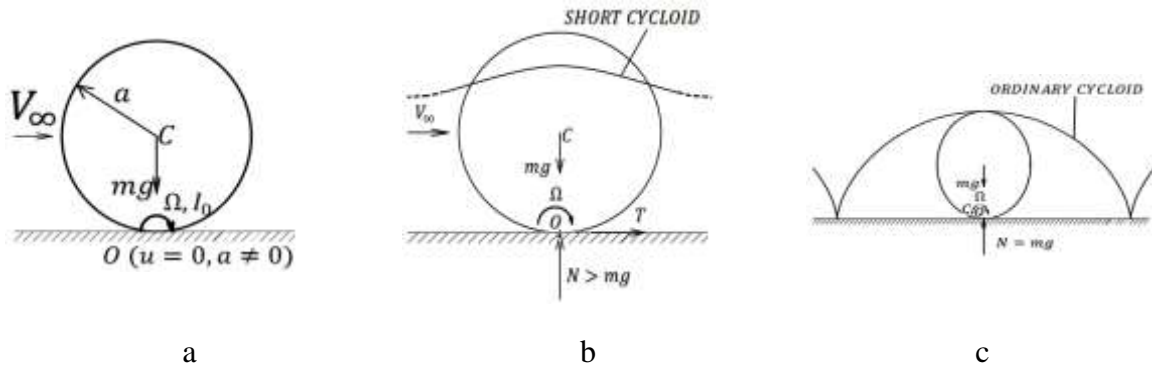
Equations (4) act as a substitute for the Stokes's hypothesis which is a condition too restricted (valid only for an elastic impact). In fact, *the CBV e^τ and viscosity v are the first and second viscosities for a thixotropic fluid.*

The post-impact motion ($t > 0$). The motion following impact is a boundary-layer structure with 2/3 translational motion and 1/3 rotational motion embedding shear concentrated vorticity at the wall, in a compact texture of laminar flow, and dispersed vorticity "en mass", i.e. the residual vorticity, across a turbulent boundary layer with a less tight texture.

The rapid loading in the contacting area of the solid boundary, during the starting, is a source where instabilities are produced and then propagated as linear/elastic and nonlinear/dispersion body waves. The local instabilities at the fluid-solid boundary interface, propagate as three wave packets/groups containing fast compressing/expanding longitudinal (L) waves and slower shearing transverse (T) waves that are mutually dependent (see § 4).

The kinematics and the dynamics of shear turbulence can be conceptually synthesized by means of the rotor-translational motion model as follows:

- The cycloidal/Legendre trajectory of a fluid particle at the wall generates itself a circular instability ($\mathbf{u}(0)=0, \mathbf{a}(0) \neq 0$) stronger than the static instability ($\mathbf{u}(0)=0, \mathbf{a}(0)=0$) in laminar flows;
- The post-starting motion develops a boundary-layer structure set up into a non-autonomous outer layer/inertial phase with the average group velocity of $\frac{V_g}{V_\infty} = \frac{2}{\pi}$, and an active autonomous inner layer/non-inertial phase at the fluid-solid boundary ($y = 0$) with the phase velocity of $\frac{V_{ph}}{V_\infty} = \frac{4}{\pi}$ (the jump of average transverse velocity) in the circular/azimuthal plane $(0, 2\pi)$;
- The wall wave packets have a phase velocity twice the group/convection velocity;
- The wave pattern is differentiated by the intensity of impact as shown in Fig. 4.



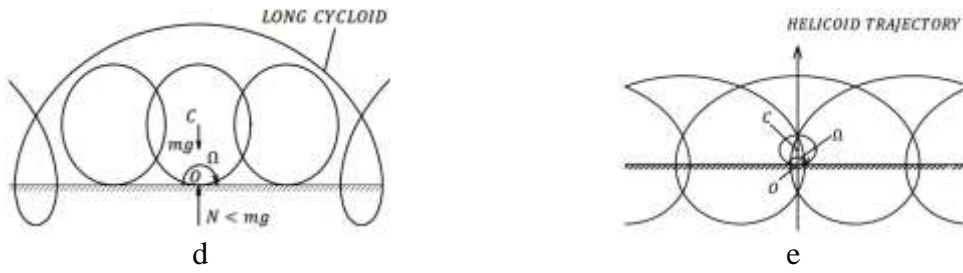


Figure 4: The causality of a plane motion (the evolution of an energy perturbation (V_∞^2) carrying a change ($I_0\Omega^2, e^{\tau\nu}$) concomitantly with its damping): a) starting impact (equal-energy partition condition; b) inelastic impact ($\lambda < 1$) with shearing friction; c) inelastic impact ($1 \leq \lambda < \lambda_1 = 3\pi/2$), steady rolling without slip; d) linear/elastic impact ($\lambda_1 \leq \lambda < \lambda_2 = 5\pi/2$), unsteady rolling/torsional elastic waves without slip; e) nonlinear/ballistic impact ($\lambda \geq \lambda_2$), unsteady rolling/nonlinear torsional waves with slip.

The intensity of a starting impact is measured by a non-dimensional normal rotational acceleration $\frac{a_n}{\Omega^2 r} \equiv \lambda$ and units of $\sqrt{g} \approx \pi$ (g is the acceleration of gravity and π is wavelength of motion), on a scale of 1 to 10. The parameter λ plays the role of a stability parameter for moving bodies in a plane motion, showing the instability level (π) closely related to the intensity of its cause \sqrt{g} (the starting impact)

$$\lambda_i = \frac{(2i+1)\pi}{2}, \text{ with } i = 1, 2, 3. \quad (5)$$

as follows:

- $\lambda_1 = 4.71$ is the Feigenbaum's criterion (4.669...) indicating the onset of the linear instability state at the molecular scale; for $\lambda \leq \lambda_1$ the impact is an inelastic impact without microstructure change.
- $\lambda_2 = 7.79$ indicates the onset of the nonlinear instability state; for $\lambda_1 < \lambda \leq \lambda_2$ the impact is a linear/elastic/random impact preserving the Gaussian behavior of the molecular microstructure without inertia changes/deformations at the macroscale;
- for $\lambda > \lambda_2$ the impact is a nonlinear/ballistic impact involving irreversible microstructure changes with nonlinear material behavior and structural damping/hysteretic (remanent deformations), [9].

Therefore, any energy perturbation propagates at high frequencies in the localized form of a three wave packet of inertial nature (a "lifting" effect, Fig. 4).

In the case of following fluids, the local stability parameter is $\log Rb$ where

- $\log Rb_{in} \equiv \log Re_{cr} = \log(v_0^{-1}) = 4.82$ is the onset of instability state;
- $\log Rb_{cr} = \log(e^2 v_0^{-1}) = 5.7 \approx 2\pi$ is the onset of transition process;
- $\log Rb_{st} = \log\left(e^{-1/2} v_0^{-\left(1+\frac{1}{2}\right)}\right) = 7.0$ is the full/statistic turbulent state.

The analogy between the stability state of solid and fluid media shows some difference in the elastic range (shorter for fluids) because of the less elasticity of incompressible flows by comparison with the solid bodies. However, the surprising similitude between the stability parameters λ and Rb , in fact both wave numbers, shows *the universal character of the starting process of a moving continuous medium*.

4 THE SHEAR VORTICITY WAVES AND SELF-SUSTAINING MECHANISM OF TURBULENCE

Commonly it is assumed that the transition process from laminar to turbulent flow occurs because of an incipient instability of the basic flow field. This non-defined instability intimately depends on subtle and obscure details of the flow [10]. Thus, the some small disturbances in the freestream enter the boundary layer from where a variety of different instabilities can occur and grow up to the breakdown of laminar flow. The scenario following various linear stability approaches within the framework of the classical Navier-Stokes theory [11], however, failed to explain the origin and the mechanism of the transition process. *The “original sin” lies just in the ignorance of the initial impulse triggering off a primary instability state*. This drawback is removed in the sense that any flow is started at some moment in time from rest, where the initial impulse/starting impact is occurred, and as long as the Reynolds number or a similar stability parameter λ doesn't exceed a critical value (Rb_{cr}, λ_2), the flow/motion remains laminar/in elastic regime. As the Reynolds number/ λ increases, some instability sets firstly in the linear/elastic range, being is followed by the transition to nonlinear instabilities, at the critical Reynolds number $Rb_{cr} = 5.69$ (or $\lambda_2 = 7.79$), and a fully developed turbulent/hysteretic damping state, Figs. 4, 10.

The transition from linear behavior to nonlinear behavior occurs when a threshold regime is attained and is closely related to the boundary singularity at $y = 0$, which in laminar regime is a static singularity ($\mathbf{u}(0) = 0, \mathbf{a}(0) = 0$), while in wall-bounded turbulent flow is a weak circular singularity with high frequency ($\mathbf{u}(0) = 0, \mathbf{a}(0) \approx \cos(\Omega t / 2 - \pi)$). The circular singularity at the contact point ($y = 0$) is analyzed in circular/azimuthal plane for a disc structure, Fig. 5.

Figure 5 shows the main differences between the models of zero-thickness inner layer ($y = 0$): inertial (fixed) material point for elastic dense structures (laminar flow) and non-inertial (free) material point for hysteretic less tight structures (turbulent flow).

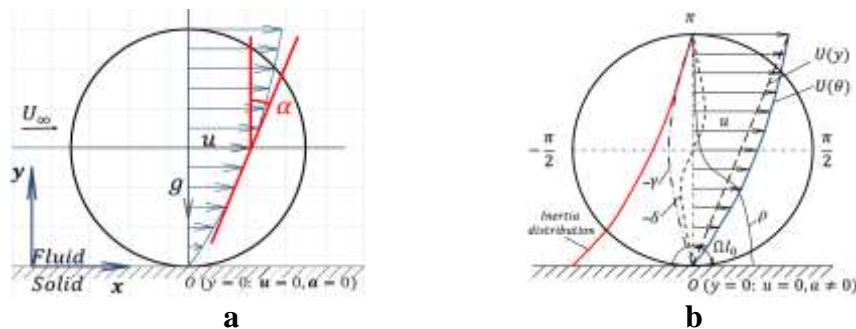


Figure 5: Local models of zero-thickness inner layer ($y = 0$): a) inertial material point in the 2D plane (zero-acceleration parallel flow model); b) non-inertial material point in the azimuthal plane (rotor-translation motion model with (ρ, γ, δ) shear waves).

As we move on from inertial rectilinear (x, y) to consider curvilinear shear flow we have defined shearing/torsion (γ) , compressing/inertia (ρ) and their rates as

$$\gamma \equiv \frac{dV(\theta, t)}{dy} = \frac{V_\infty}{4a \sin \theta/2} = \Omega \frac{1}{2 \sin \theta/2}, \quad (6a)$$

$$\dot{\gamma} \equiv \frac{d\gamma}{dt} = \Omega^2 \frac{\cos \theta/2}{\sin^2 \theta/2}, \quad (6b)$$

$$\rho \equiv I(\theta, t)\Omega = a^2 \Omega \frac{3}{2} \cos^3 \frac{\theta}{2}, \quad (6c)$$

$$\dot{\rho} \equiv \frac{d\rho}{dt} = -\frac{9}{8} a \Omega^2 \cos \theta/2 \sin \theta. \quad (6d)$$

From Eqs. (6a) and (6b) we can obtain the torsion degree τ of the wall-bounded flow as

$$\tau \equiv \frac{1}{\Omega} \frac{d}{dt} (\ln \gamma) = 2 \cot \frac{\theta}{2}. \quad (7)$$

where for $\theta \geq \pi/2$ and $\tau \leq 2$ the torsion is linear while for $\theta \geq \pi/2$ and $\tau > 2$ the torsion is nonlinear. Apart from some dimensional constants the shearing (γ) , compressing (ρ) and the mutual dispersion function $\delta(\dot{\gamma} \leftrightarrow \dot{\rho})$ represent dynamic processes with high frequency on different azimuthal mode shapes in the form of three coupled shear waves: the elastic shear wave (γ) , inertial compressing wave (ρ) and dispersion wave (δ) induced by the circular/azimuthal boundary singularity. In fact, the shear waves (ρ, γ, δ) are respectively, transport, relative and Coriolis components of acceleration $\mathbf{a}(0)$ of the non-inertial/free point $y = 0$ ($\mathbf{u}(0) = 0, \mathbf{a}(0) \neq 0$), physically describing distinct states of twisted vorticity as pressure (ρ) membrane (γ) and spray (δ) .

The shear waves lie in the origin of coherent structures in shear flows and their dynamics is associated with the phenomenon of bursting [12] (see Fig. 6).

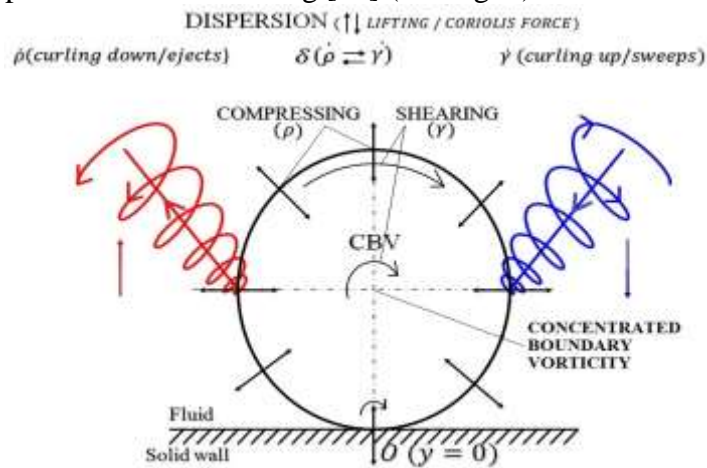


Figure 6: Local coupling of shearing (γ), compressing (ρ) and dispersion (δ) (self-sustaining mechanism of wall turbulence).

A priori transition, wave number $k < k_{tr}$, the dispersion process can be ignored and the local dynamic balance between “shearing elastic force (γ)” and “compressing inertial force (ρ)” is described kinematically by linear torsional vibrations

$$\ddot{\tau} + k^2 \tau = 0, \quad (8)$$

with the wave number $k < k_{tr} = 2\pi$ and the torsion index $\tau < 2$.

At the transition $k \geq k_{tr}$, the starting impact is a ballistic one where the twist of contact structure exceeds 2π , followed by fluid microstructure changes with a nonlinear/hysteretic damping behavior (i.e. non Gaussian) of twisted boundary vorticity and an abrupt intensifying of dispersion process (δ) on account of the intrinsic energy (compressing “latent” heat) of fluid. All coupled processes (shearing, compressing and dispersion) are running as a whole (the self-sustaining mechanism of turbulence) up to the point where the starting energy perturbation (e^2) is offset/damped by its dispersion and embedding in a new microstructure of fluid (compressible fluid at $Re_{indiff} \approx 10^8$). The dispersion process is a sort of inertial Coriolis force producing intermittent lifting effects as sketched in Fig. 6.

The local dynamic balance between the fast shearing, hysteretic compressing and dispersion processes can be kinematically described in phase plane by the nonlinear equation (9) of the torsion pendulum with hysteretic damping, Fig. 7.

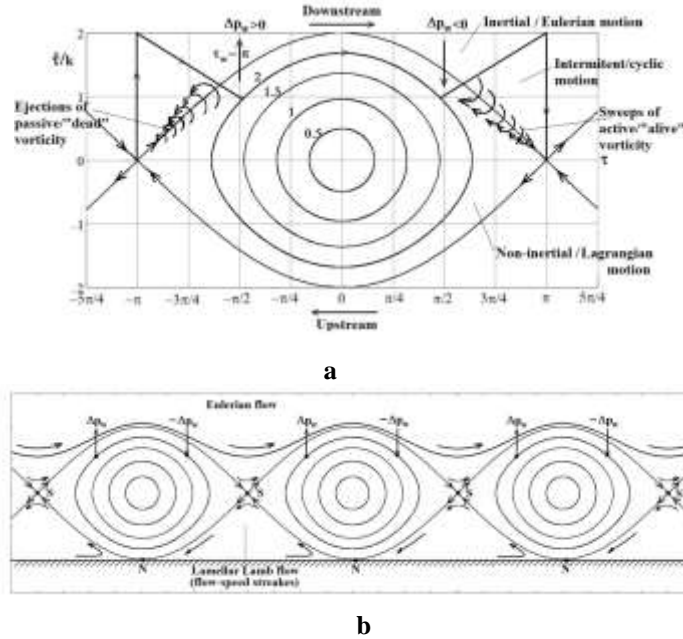


Figure 7: The fundamental “cat-eyes” coherent structures (CES) at the wall: a) torsion pendulum mechanism: phase curves and separatrix ($\tau_m = \pi$) of motions in the phase plane; b) topology of wall-bounded motion in the azimuthal plane ($y = 0$) and the bursting phenomenon (Δp_w - jump of wall pressure).

$$\ddot{\tau} + k^2 \sin \tau = 0, \quad (9)$$

where the limit of small amplitudes $\tau_m \leq 2$ renders the linearized solution and constant period $T_l = 2\pi/\Omega = 10^{-k}$. In the phase plane ($\dot{\tau}/k(\tau)$) a limit cycle exists for $\tau_m < \pi$, indicating a rotational motion, while the solution for $\tau_m > \pi$ is no longer closed and is extended to infinity as a translational motion. A separatrix for $\tau_m = \pi$ in the phase plane, separates the two kinds of motion (Fig. 7a), [2].

Note that the most primary concentrated vorticity (e^r) structure nearest the wall ($y = 0$), moving independently from the streamlines (translation motion), is a “cat-eyes”-like coherent structure (CES), educed from Eq. 9, Fig. 7b. The CES is the fast inertial/compressing wave (ρ) of Lagrangian nature, extracting the molecular thermal energy of fluid for the sustenance of the slower shear (γ) and dispersion (δ) waves. The whole shear wave packet, i.e. the soliton coherent structure (SCS) penetrates then the outer inertial layer activating the wall-bounded flow.

The parametric evolution of the transition process, from laminar to turbulent flow in the Prandtl boundary layer flow, can be visualized by means of the similar soliton solutions [2], (Fig. 8) and the generalized Stokes’s hypothesis from Eqs. 4. It is worth marking that at $Re_l = 10^7$, the separatrix of motions is achieved (a wall effect termed “intrinsic/molecular slip”) and further the Reynolds number is practically indifferent towards flow and the local isotropy is restored.

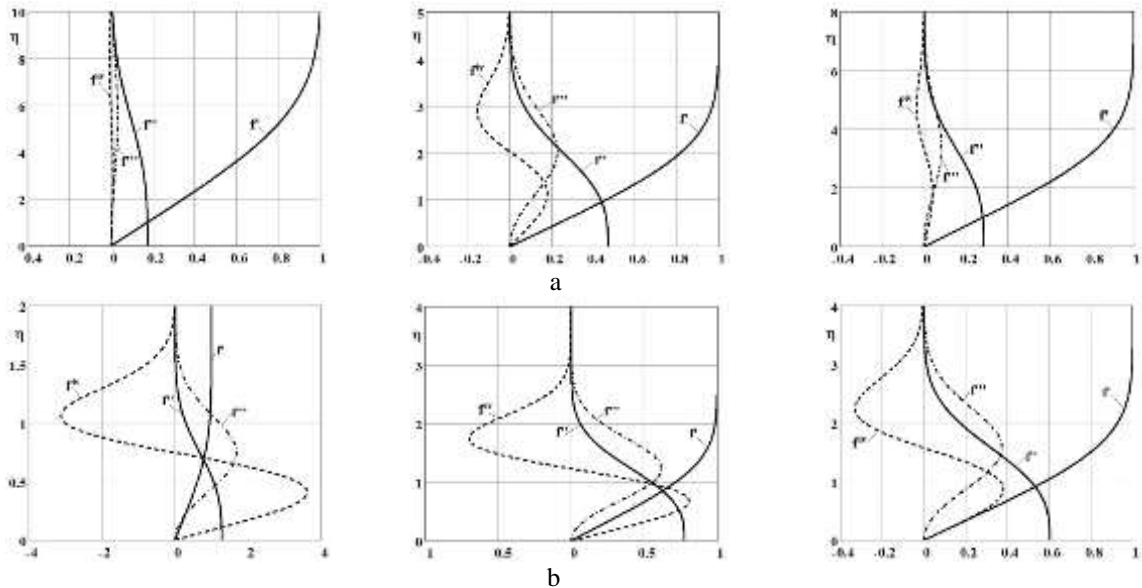


Figure 8: Similar soliton solutions of mean velocity and shear wave fields with a generalized Stokes’s hypothesis (Eqs. 4) for the Prandtl boundary-layer flow: a) laminar flows (linear/elastic impact):

$$Rb = e^0 v_0^{-1} (\approx 10^5) - e^2 v_0^{-1} (\approx 5 \cdot 10^5); \text{ b) transitional-turbulent flows (nonlinear/ballistic impact):}$$

$$Rb = e^{-\frac{2}{3}} v_0^{-\left(1+\frac{1}{3}\right)} (\approx 10^6), e^{-\frac{1}{2}} v_0^{-\left(1+\frac{1}{2}\right)} (\approx 10^7), e^{-\frac{1}{3}} v_0^{-\left(1+\frac{2}{3}\right)} (\approx 10^8).$$

5 CONCLUSIONS

The paper presents an unitary approach of the plane motions strained by boundaries for a continuous medium, fluid or solid. The key hypothesis for such motions is the fact that the onset

of motion is a kind of impact (starting impact) which governs the subsequent evolution of motion. The starting impact is an energy perturbation localized in a wave packet at the fluid-solid boundary interface, which has the important advantage concerning the transport of the perturbation energy concomitantly with its damping. The ignorance of this initial impulse as a twisted contact structure triggering off further instabilities (bifurcations), followed by transition and a hysteretic damping, led to a branching in the phenomenology of turbulence which sometimes obscured physical and mathematical justification.

The present approach follows a direct reasoning from the origin/causes (twisted contact structure) to diverse facts/effects where in the case of complicated turbulence phenomenon, the ignorance of its causes gave birth, in exchange to, a number of beautiful images of turbulent flows easily observed, but extremely difficult to interpret, understand and explain.

By means of the model of starting impact-rotor translational motion at the wall, the paper proposes a universal stability criterion/parameter which governs the stability state along the successive development of motion, from the origin up to when an ultimate (statistical) state is restored. Thus, the transition process becomes a well-defined state as the jump from linear (twist $< 2\pi$) to nonlinear (twist $\geq 2\pi$) behavior for both solid and fluid plane motions.

REFERENCES

- [1] Reynolds, O. Study of fluid motion by means of colored bands, *Nature*, **50**, pp. 161-164, (1894).
- [2] Dumitrescu, H. and Cardos, V. The origin of shear turbulence, *INCAS Bulletin*, Volume 9, Issue 4, pp. 75-89, (2017).
- [3] Lee, C.B. and Wu, J.Z. Transition in wall-bounded flows, *Applied Mechanics Reviews*, C 1, 030802, (2008).
- [4] Wu, J.Z., Ma, H.Y. and Zhou, M.D. *Vortical Flows*, Springer Verlag Science+Business Media, (2015).
- [5] Stokes, G.G. On the theories of internal friction of fluids in motion, *Trans Cambr. Phil. Soc.*, **8**, pp. 287-305, (1845).
- [6] Tsinober, A. *The Essence of Turbulence as a Physical Phenomenon*, Springer Dordrecht Heidelberg, New York, London, (2014).
- [7] Prandtl, L. Über Flüssigkeitsbewegung bei sehr kleiner Reibung, Heidelberg: *Proceedings of the III International Mathematics Congress*, (1904)
- [8] Stuart, T. J. On finite amplitude oscillations in laminar mixing layers, *Journal of Fluid Mechanics*, **29**, part 3, 417-440, (1967).
- [9] Corwin, I. Kardar-Parisi-Zhang (KPZ) universality, *EMS Newsletter*, No. **101**, September, pp. 19-27, (2016).
- [10] Klewichi, J.C., Saric, W.S., Marusic, I., Eaton, J.K. *Wall-bounded flows*, In *Handbook of experimental fluid mechanics*, Springer, pp. 871-902, (2007).
- [11] Ladyzhenskaja, O.A. *Mathematical problems of the dynamics of viscous incompressible fluids*, Gordon and Beach, New York, (1969).
- [12] Kline, S.J., Reynolds, W.C., Schraub, F.A., Runstadler, P.W. The structure of turbulent boundary layers, *Journal of Fluid Mechanics*, **30**, pp. 741-773, (1967).